


Timescales of Quantum Equilibration, Dissipation and Fluctuation in Nuclear CollisionsC. Simenel^{✉*}*Department of Theoretical Physics and Department of Nuclear Physics, Research School of Physics and Engineering,
The Australian National University, Canberra ACT 2601, Australia*K. Godbey^{✉†‡} and A. S. Umar^{✉‡}*Department of Physics and Astronomy, Vanderbilt University, Nashville, Tennessee 37235, USA* (Received 25 March 2020; revised manuscript received 2 May 2020; accepted 8 May 2020; published 27 May 2020)

Understanding the dynamics of equilibration processes in quantum systems as well as their interplay with dissipation and fluctuation is a major challenge in quantum many-body theory. The timescales of such processes are investigated in collisions of atomic nuclei using fully microscopic approaches. Results from time-dependent Hartree-Fock and time-dependent random-phase approximation calculations are compared for 13 systems over a broad range of energies. The timescale for full mass equilibration ($\sim 2 \times 10^{-20}$ s) is found to be much larger than timescales for neutron-to-proton equilibration, kinetic energy, and angular momentum dissipations which are on the order of 10^{-21} s. Fluctuations of mass numbers in the fragments and correlations between their neutron and proton numbers build up within only a few 10^{-21} s. This indicates that dissipation is basically not impacted by mass equilibration, but is mostly driven by the exchange of nucleons between the fragments.

DOI: [10.1103/PhysRevLett.124.212504](https://doi.org/10.1103/PhysRevLett.124.212504)

It is well known that two classical systems with differing properties (e.g., two fluids of different colors or temperatures) that are able to exchange matter in some way tend to equilibrate their initial asymmetry over time. This equilibration process also occurs in quantum systems, a phenomenon actively studied at present with quantum simulations using ultracold atoms and trapped ions [1]. The principal challenge is in characterizing the path followed by a quantum system as it evolves towards equilibrium. Along this path, the system also encounters dissipation of collective energy (e.g., kinetic energy of collision partners) into internal degrees of freedom. Although equilibration processes are expected to depend on dissipative mechanisms, the interplay between equilibration and dissipation in quantum systems is still not well understood.

Collisions of atomic nuclei are ideal to investigate equilibration and dissipative processes in quantum many-body systems [2,3]. Indeed, these collisions are usually too fast (on the order of a few zeptoseconds, $1 \text{ zs} = 10^{-21}$ s) to allow interaction with external environment to affect the outcome of the collision. For example, emission of γ photons due to coupling to the electromagnetic field occurs over a much longer timescale, usually greater than 10^{-18} s. Nevertheless, nucleons, which move at about 20% speed of light in the nucleus can be transferred from one nucleus to the other when the nuclei are in contact. As a result, the internal degrees of freedom characterising the nuclear states encounter a rapid rearrangement, tending to equalize initial asymmetries between the collision partners as well as

dissipating their kinetic energy and angular momentum. In addition, the relatively small number of nucleons at play (up to a few hundred) makes the problem numerically tractable if one makes relevant approximations to the quantum many-body problem.

The mass (number of nucleons) of the nuclei and the difference between their neutron and proton numbers are among the main collective degrees of freedom which can encounter equilibration in heavy-ion collisions. A broad range of masses, and thus chemical potentials, are already accessible with stable beams. Moreover, the recent development of exotic beams has significantly increased the range of available asymmetries between protons and neutrons, leading to ambitious reaction mechanism programs at exotic beam facilities around the world, including FRIB (U.S.) [4], RIKEN-RIBF (Japan) [5], SPIRAL2 (France) [6], and FAIR-NUSTAR (Germany) [7]. In particular, neutron-proton asymmetric collisions are expected to bring valuable information on the density dependence of the nuclear symmetry energy, which is highly relevant in nuclear astrophysics (see [8] for a recent review).

As mass and neutron-proton equilibration occurs via a flow of nucleons between colliding partners, they are expected to be significantly impacted by nuclear viscosity. The latter is also responsible for dissipation of both the initial kinetic energy and the angular momentum of the fragments [9]. In turn, as a manifestation of Einstein's fluctuation-dissipation theorem, the multinucleon transfer between the fragments in contact is expected to build up quantum fluctuations that lead to broad distributions of

particle numbers in the final fragments [10]. Equilibration, dissipation, and fluctuation then form a complex network of interrelated observables.

Investigating the interplay between these quantities requires advanced theoretical descriptions. We adopt fully microscopic time-dependent approaches to the nuclear many-body problem allowing for parameter-free (except for the underlying nuclear interaction) dynamical descriptions of the relevant quantities (see [11–13] for recent reviews). The number of transferred nucleons, the kinetic energy of the fragments, and their angular momenta are all described by one-body observables. Average values of these quantities are computed with the time-dependent Hartree-Fock (TDHF) mean-field theory, which is optimized for expectation values of one-body operators [14]. In particular, TDHF contains all one-body dissipation mechanisms which are the most relevant at the energies considered in this work (see, e.g., discussion in [11]). However, TDHF often underestimates fluctuations of these operators [15,16]. We thus compute fluctuations of neutron and proton numbers (as well as their correlations) in the fragments from the time-dependent random-phase approximation (TDRPA) prescription of Balian and Vénéroni [17], which is indeed optimized on fluctuations of one-body operators in the limit of small fluctuations.

Probably the most important quantity characterizing various equilibration, dissipation, and fluctuation processes is the timescale over which they occur. A first step is then to investigate these timescales, their potential dependence on the entrance channel, and compare them to understand their relationships. Indeed, mechanisms with very different timescales are unlikely to be correlated while similar timescales indicate a potential common origin in the underlying microscopic mechanisms. In this letter we present a systematic theoretical study of timescales for mass and neutron-proton equilibration and fluctuations, as well as kinetic energy and angular momentum dissipation. TDHF and TDRPA results are presented for many collisions spanning a broad range of masses, energies and angular momenta (see the Supplemental Material [18]). Although most results are compiled from published data, we have performed new calculations for completeness with the TDHF3D code [19] for $^{40}\text{Ca} + ^{40,48}\text{Ca}$, ^{64}Ni (see, e.g., [20] for numerical details) and with the code of Ref. [21] for $^{176}\text{Yb} + ^{176}\text{Yb}$. These new calculations used the SLy4d parametrization of the energy density functional [19].

In order to compare various systems with different initial conditions, let us introduce a generic way of defining a “normalized” observable $\delta X(\tau) = [X(\tau) - X_\infty]/(X_0 - X_\infty)$ where $X(\tau)$ is the quantity used to characterise equilibration, dissipation or fluctuations. It is a function of the contact time τ between the fragments before they reseparate. Here, contact is usually defined by two fragments linked by a neck, with a neck density exceeding half the saturation density $\rho_{\text{sat}}/2 \simeq 0.08 \text{ fm}^{-3}$. The initial value

of X is noted X_0 . For long contact times, the value of X is expected to saturate to its equilibrium value X_∞ , in which case $\delta X \rightarrow 0$. For quasielastic collisions in which contact does not occur (with the above definition of contact), the contact time is obviously $\tau = 0$, leading to $\delta X(0) = 1$. However, the nuclei may interact before contact through the overlap of their density tails, possibly leading to values of $\delta X(0) \neq 1$.

Equilibration of mass asymmetry $\delta\Delta A(\tau)$ is studied in Fig. 1 with $\Delta A \equiv A_1 - A_2$ and $A_{1,2}$ the number of nucleons in the outgoing fragments obtained from a series of TDHF calculations [22–25] for systems at energies near the Coulomb capture barrier V_B [26]. For each system and energy, a range of angular momenta is considered, thus producing a distribution of contact times with various exit channels. Note that each point typically requires several days of computational time on modern computers. The equilibrium value for mass asymmetry is chosen to be $\Delta A_\infty = 0$, i.e., with two outgoing fragments of similar masses. Note that this equilibrium is rarely reached due to shell effects in the fragments favoring exit channels before full symmetry is achieved [24,27,28]. Despite large fluctuations of $\delta\Delta A(\tau)$, all systems exhibit a similar pattern, with an equilibration of mass asymmetry and a full symmetry expected to be reached at about 20 zs contact time in average. This indicates that mass equilibration is a relatively slow process. Such reactions are called quasi-fission [29] as fissionlike fragments are produced without formation of an intermediate compound nucleus (which would require much longer time). These TDHF predictions of mass equilibration times are in good agreement with “neutron clock” [30] and fragment mass-angle distribution [29,31,32] measurements.

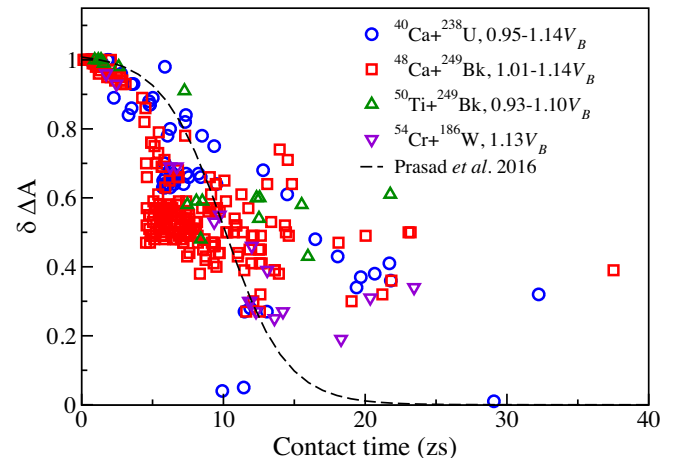


FIG. 1. Fragment mass asymmetry as a function of contact times from TDHF calculations of $^{40}\text{Ca} + ^{128}\text{U}$ [22], ^{48}Ca , $^{50}\text{Ti} + ^{249}\text{Bk}$ [23,24], and $^{54}\text{Cr} + ^{186}\text{W}$ [25]. Energy ranges are given as function of the barrier height V_B [26]. The dashed line shows the expected equilibration assuming Fermi-type mass drift determined experimentally by Prasad *et al.* [31].

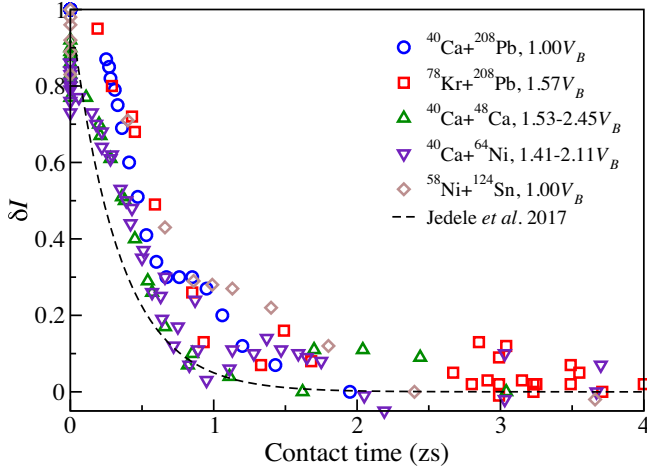


FIG. 2. Asymmetry between proton and neutron numbers as a function of contact times from TDHF calculations of $^{40}\text{Ca} + ^{208}\text{Pb}$ [33], $^{78}\text{Kr} + ^{208}\text{Pb}$ [34], $^{40}\text{Ca} + ^{48}\text{Ca}$, ^{64}Ni (this work), and $^{58}\text{Ni} + ^{124}\text{Sn}$ [35]. Energy ranges are given as function of the barrier height V_B [26]. The dashed line shows the expected equilibration assuming the rate constant of 3 zs^{-1} determined experimentally by Jedele *et al.* [36].

We now investigate equilibration of initial asymmetry between proton and neutron numbers, quantified by $I = (N_1 - Z_1) - (N_2 - Z_2)$, with $Z_{1,2}$ the number of protons and $N_{1,2} = A_{1,2} - Z_{1,2}$ the number of neutrons in the fragments. Figure 2 shows $\delta I(\tau)$ for various systems studied with TDHF [33–35]. Here, the equilibrium values I_∞ are smaller (in magnitude) than I_0 , though not necessarily zero, and I_∞ needs to be determined for each system. This is done by taking $I(\tau)$ for large times when it does not significantly change with τ anymore. The fact that we usually have $I_\infty \neq 0$ (see, e.g., Fig. 10 of Ref. [34]) is essentially due to the remaining charge (Z) asymmetry which favors different values of $N - Z$ in the fragments because of different Coulomb energies. We see in Fig. 2 that neutron-proton equilibration is a much faster phenomenon than mass equilibration as $\delta I(\tau)$ is approximately zero for $\tau \sim 1 \text{ zs}$ and above. This timescale is in good agreement with what has been recently determined experimentally from reactions at intermediate energies [36] (dashed line in Fig. 2).

Next, we investigate the timescale for dissipation of total kinetic energy (TKE) of the fragments. This usually involves reactions well above the barrier, in which collision terms (not included in TDHF) could affect the reaction mechanisms. Nevertheless, the fact that fully damped collisions are obtained in TDHF [13,23,24,34,35,37,38], together with comparison between TKE predictions and experimental data [37], indicate that one-body dissipation mechanisms (the only ones included in TDHF) are sufficient up to these energies. Fully damped collisions have a value of TKE_∞ which depends on the system. It roughly corresponds to the Coulomb repulsion between the

fragments at scission, and is usually well approximated by Viola systematics [39,40]. However, the final TKE for a given system can also be affected by initial conditions such as the orientation of a deformed collision partner in the entrance channel [23]. Therefore, we determine the value of TKE_∞ for each system and each energy (when a broad range of energies is considered).

The resulting $\delta \text{TKE}(\tau)$, as predicted by TDHF calculations [23,24,34,35,37,38], are shown in Fig. 3. A full dissipation is obtained after typically 1–2 zs, indicating a fast process with similar timescale as in neutron-to-proton equilibration. Experimentally, a possible way to extract timescales is through fragment angular distributions. Recent TDHF predictions of TKE-angle correlations in $^{58}\text{Ni} + ^{60}\text{Ni}$ deep-inelastic collisions have been found to be in good agreement with experiment [37], supporting our extracted timescale for energy dissipation.

We also investigated dissipation of orbital angular momentum L between the fragments. Let us define $L_{\text{loss}}(\tau) = L_0 - L(\tau)$ as the difference between initial and final angular momentum, giving $L_{\text{loss}0} = 0$. The behavior of $L_{\text{loss}}(\tau)$ for a given system at a given energy (i.e., varying only L_0), is first to rise with τ due to dissipation, and then to decrease slowly at large contact times, as the latter correspond to more central collisions, i.e., with less initial angular momentum L_0 available for dissipation. We thus define the equilibrium value $L_{\text{loss}\infty}$ as the maximum value of $L_{\text{loss}}(\tau)$. Figure 4 shows the resulting evolution of δL_{loss} with contact time for a set of reactions studied with TDHF [11,34,38,41]. Note that

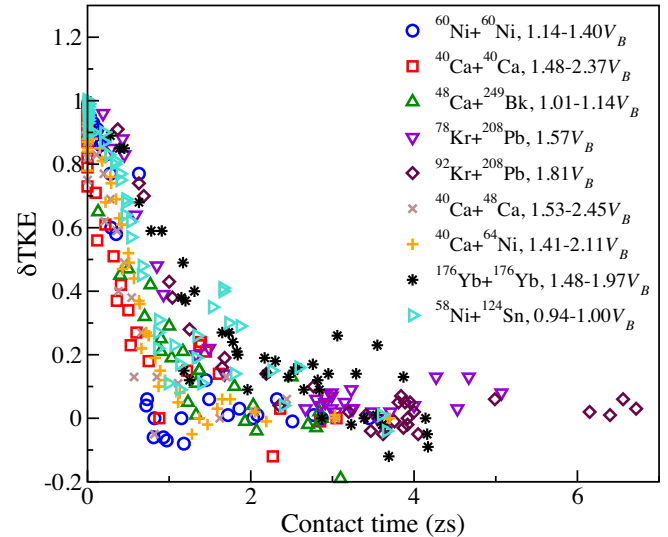


FIG. 3. Evolution of δTKE as a function of contact times from TDHF calculations of $^{60}\text{Ni} + ^{60}\text{Ni}$ [37], $^{40}\text{Ca} + ^{40}\text{Ca}$ [38] (and this work), $^{48}\text{Ca} + ^{249}\text{Bk}$ [23,24], $^{78,92}\text{Kr} + ^{208}\text{Pb}$ [34], $^{40}\text{Ca} + ^{48}\text{Ca}$, ^{64}Ni (this work), $^{176}\text{Yb} + ^{176}\text{Yb}$ [41] (and this work), and $^{58}\text{Ni} + ^{124}\text{Sn}$ [35]. Energy ranges are given as function of the barrier height V_B [26].

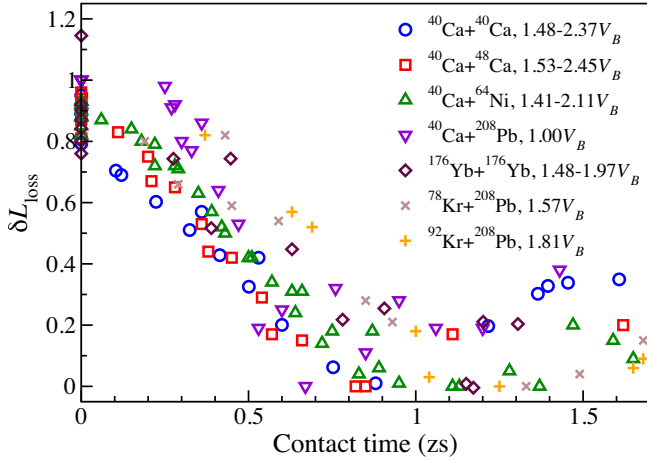


FIG. 4. Evolution of δL_{loss} as a function of contact times from TDHF calculations of $^{40}\text{Ca} + ^{40}\text{Ca}$ [38] (and this work), $^{40}\text{Ca} + ^{48}\text{Ca}$, ^{64}Ni (this work), $^{40}\text{Ca} + ^{208}\text{Pb}$ [11], $^{176}\text{Yb} + ^{176}\text{Yb}$ [41] (and this work), and $^{78,92}\text{Kr} + ^{208}\text{Pb}$ [34]. Energy ranges are given as function of the barrier height V_B [26].

$\delta L_{\text{loss}} > 1$ is sometimes observed for collisions of deformed nuclei that allow transfer from intrinsic to orbital angular momentum. Nevertheless, most reactions have dissipated their angular momentum within 1 zs.

Let us finally study the dynamics of mass fluctuations $\sigma_A = \sqrt{\langle \hat{A}^2 \rangle - \langle \hat{A} \rangle^2}$ and proton-neutron correlations $\sigma_{NZ} = \sqrt{\langle \hat{N} \hat{Z} \rangle - \langle \hat{N} \rangle \langle \hat{Z} \rangle}$, where \hat{A} , \hat{N} , and \hat{Z} count particles in the fragments. These fluctuations and correlations have been determined with TDRPA in deep inelastic collisions (DIC) [37,38,41]. These systems are symmetric to avoid possible spurious effects due to skewed fragment mass distributions, which may occur in asymmetric systems, and which prevent the interpretation of TDRPA results as fluctuations [37]. As the particle numbers in the incoming fragments are well defined, we have $\sigma_{A_0} = \sigma_{NZ_0} = 0$. It is also found that, in most central DIC, TDRPA fluctuations exhibit relatively large fluctuations around an average value which we choose for $\sigma_{A,\infty}$.

The evolutions of $\delta\sigma_A(\tau)$ and $\delta\sigma_{NZ}(\tau)$ as a function of contact time are shown in Fig. 5. The observed decrease of $\delta\sigma_A(\tau)$ and $\delta\sigma_{NZ}(\tau)$ indicates that fluctuations and correlations build up within a timescale of about 3 zs. Naturally, the choices of $\sigma_{A,\infty}$ and $\sigma_{NZ,\infty}$ are quite arbitrary, and changing these values would impact the slopes of $\delta\sigma(\tau)$. Nevertheless, as all three systems reach their maximum fluctuations at similar contact times, this would not have a significant influence on the resulting timescales. However, the small number of systems, together with the large variations of fluctuations due to the sensitivity to initial condition in DIC, prevent to draw definitive conclusions with respect to the universality of the behavior of mass fluctuations. More studies would be welcome.

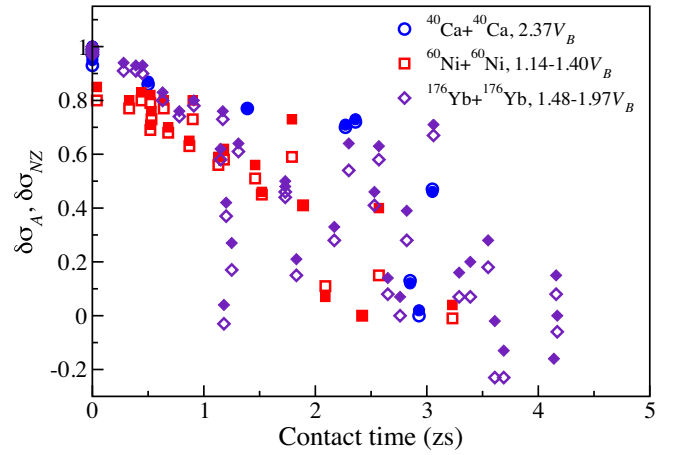


FIG. 5. Evolution of $\delta\sigma_A$ associated with mass fluctuations (open symbols) and $\delta\sigma_{NZ}$ associated with neutron-proton correlations (full symbols) as a function of contact times from TDRPA calculations of $^{40}\text{Ca} + ^{40}\text{Ca}$ [38] (and this work), $^{60}\text{Ni} + ^{60}\text{Ni}$ [37], and $^{176}\text{Yb} + ^{176}\text{Yb}$ [41] (and this work). Energy ranges are given as function of the barrier height V_B [26].

A comparison between the different timescales for equilibration, dissipation, and fluctuation processes leads to several conclusions. First, it is quite remarkable that each process exhibits similar timescales despite being derived from extremely different systems and energies. This is a strong indication that the underlying mechanisms are universal and do not depend much on the specifics of the entrance channel. Note that the present systematics also include calculations by several teams with different TDHF [19,21,42–44] and TDRPA [37,38,41] codes and two different energy density functionals [19,45], showing the robustness of the results.

Second, it is noticeable that neutron-to-proton equilibration occurs on very similar timescales as angular momentum and kinetic energy dissipations. This points toward a strong correlation between these mechanisms. However, neutron-to-proton equilibration cannot be the sole dissipative mechanism as collisions in systems with neutron-to-proton symmetry have a similar timescale for dissipation (see Fig. 3).

The main mechanism for dissipation is expected to be multinucleon transfer between the fragments [10]. The least bound nucleons (closest to the Fermi surface) are usually more freely transferred. In neutron-to-proton asymmetric systems, this essentially leads to protons flowing one way and neutrons being transferred the other way. In the case of symmetric systems, however, protons and/or neutrons flow both ways. If the corresponding timescale is the same as for neutron-to-proton equilibration, this would explain why dissipation timescales are the same in neutron-to-proton symmetric and asymmetric systems.

Another observation is that mass equilibration is much slower (by more than one order of magnitude) than dissipation. It takes place in systems in which energy

and angular momentum have already been damped. From this separation of timescales we can conclude that mass equilibration is not expected to be a significant contributor to dissipation processes.

Finally, the fluctuations and correlations in particle numbers build up within a few zeptoseconds, which is a bit slower than dissipation. Nevertheless, it is still much faster than mass equilibration. Note, however, that TDRPA predictions of fluctuations are only available for symmetric systems. The increase of mass fluctuations with contact time in symmetric collisions is a clear signature that multinucleon transfer has happened (both ways due to symmetry) within this time frame. It would be interesting to investigate timescales for fluctuations and correlations in asymmetric systems with beyond TDRPA models such as the stochastic mean-field approach [46].

We thank D. J. Hinde for useful discussions. This work has been supported by the Australian Research Council Discovery Project (Projects No. DP160101254 and No. DP190100256) funding schemes and by the U.S. Department of Energy under Grant No. DE-SC0013847 with Vanderbilt University. The calculations have been performed in part at the NCI National Facility in Canberra, Australia, which is supported by the Australian Commonwealth Government.

*cedric.simenel@anu.edu.au

†kyle.s.godbey@vanderbilt.edu

‡umar@compsci.cas.vanderbilt.edu

- [1] J. Eisert, M. Friesdorf, and C. Gogolin, Quantum many-body systems out of equilibrium, *Nat. Phys.* **11**, 124 (2015).
- [2] L. G. Moretto and R. P. Schmitt, Deep inelastic reactions: A probe of the collective properties of nuclear matter, *Rep. Prog. Phys.* **44**, 533 (1981).
- [3] V. E. Viola, Nucleus-nucleus collisions: A laboratory for studying equilibration phenomena, *Acc. Chem. Res.* **20**, 32 (1987).
- [4] T. Glasmacher, B. Sherrill, W. Nazarewicz, A. Gade, P. Mantica, J. Wei, G. Bollen, and B. Bull, Facility for Rare Isotope Beams Update for Nuclear Physics News, *Nucl. Phys. News* **27**, 28 (2017).
- [5] H. Sakurai, Nuclear reaction and structure programs at RIKEN, *Nucl. Phys.* **A834**, 388c (2010).
- [6] M. Lewitowicz, The SPIRAL2 project and experiments with high-intensity rare isotope beams, *J. Phys. Conf. Ser.* **312**, 052014 (2011).
- [7] N. Kalantar-Nayestanaki and A. Bruce, NUSTAR: Nuclear Structure Astrophysics and Reactions at FAIR, *Nucl. Phys. News* **28**, 5 (2018).
- [8] A. B. McIntosh and S. J. Yennello, Interplay of neutron-proton equilibration and nuclear dynamics, *Prog. Part. Nucl. Phys.* **108**, 103707 (2019).
- [9] J. Randrup, Transport of angular momentum in damped nuclear reactions, *Nucl. Phys.* **A383**, 468 (1982).
- [10] J. Randrup, Mass transport in nuclear collisions, *Nucl. Phys.* **A307**, 319 (1978).
- [11] C. Simenel, Nuclear quantum many-body dynamics, *Eur. Phys. J. A* **48**, 152 (2012).
- [12] C. Simenel and A. S. Umar, Heavy-ion collisions and fission dynamics with the time-dependent Hartree-Fock theory and its extensions, *Prog. Part. Nucl. Phys.* **103**, 19 (2018).
- [13] K. Sekizawa, TDHF theory and its extensions for the multinucleon transfer reaction: A mini review, *Front. Phys.* **7**, 20 (2019).
- [14] R. Balian and M. Vénéroni, Time-Dependent Variational Principle for Predicting the Expectation Value of an Observable, *Phys. Rev. Lett.* **47**, 1353 (1981).
- [15] S. E. Koonin, K. T. R. Davies, V. Maruhn-Rezwani, H. Feldmeier, S. J. Krieger, and J. W. Negele, Time-dependent Hartree-Fock calculations for $^{16}\text{O} + ^{16}\text{O}$ and $^{40}\text{Ca} + ^{40}\text{Ca}$ reactions, *Phys. Rev. C* **15**, 1359 (1977).
- [16] C. H. Dasso, T. Dossing, and H. C. Pauli, On the mass distribution in time-dependent Hartree-Fock calculations of heavy-ion collisions, *Z. Phys. A* **289**, 395 (1979).
- [17] R. Balian and M. Vénéroni, Fluctuations in a time-dependent mean-field approach, *Phys. Lett.* **136B**, 301 (1984).
- [18] See the Supplemental Material at <http://link.aps.org/supplemental/10.1103/PhysRevLett.124.212504> for an extended discussion of the calculations presented in this work.
- [19] K.-H. Kim, T. Otsuka, and P. Bonche, Three-dimensional TDHF calculations for reactions of unstable nuclei, *J. Phys. G* **23**, 1267 (1997).
- [20] C. Simenel and B. Avez, Time-dependent Hartree-Fock description of heavy ions fusion, *Intl. J. Mod. Phys. E* **17**, 31 (2008).
- [21] A. S. Umar and V. E. Oberacker, Three-dimensional unrestricted time-dependent Hartree-Fock fusion calculations using the full Skyrme interaction, *Phys. Rev. C* **73**, 054607 (2006).
- [22] V. E. Oberacker, A. S. Umar, and C. Simenel, Dissipative dynamics in quasifission, *Phys. Rev. C* **90**, 054605 (2014).
- [23] A. S. Umar, V. E. Oberacker, and C. Simenel, Fusion and quasifission dynamics in the reactions $^{48}\text{Ca} + ^{249}\text{Bk}$ and $^{50}\text{Ti} + ^{249}\text{Bk}$ using a time-dependent Hartree-Fock approach, *Phys. Rev. C* **94**, 024605 (2016).
- [24] K. Godbey, A. S. Umar, and C. Simenel, Deformed shell effects in $^{48}\text{Ca} + ^{249}\text{Bk}$ quasifission fragments, *Phys. Rev. C* **100**, 024610 (2019).
- [25] K. Hammerton, Z. Kohley, D. J. Hinde, M. Dasgupta, A. Wakhle, E. Williams, V. E. Oberacker, A. S. Umar, I. P. Carter, K. J. Cook, J. Greene, D. Y. Jeung, D. H. Luong, S. D. McNeil, C. S. Palshetkar, D. C. Rafferty, C. Simenel, and K. Stiefel, Reduced quasifission competition in fusion reactions forming neutron-rich heavy elements, *Phys. Rev. C* **91**, 041602(R) (2015).
- [26] W. J. Świątecki, K. Siwek-Wilczyńska, and J. Wilczyński, Fusion by diffusion. II. Synthesis of transfermium elements in cold fusion reactions, *Phys. Rev. C* **71**, 014602 (2005).
- [27] A. Wakhle, C. Simenel, D. J. Hinde, M. Dasgupta, M. Evers, D. H. Luong, R. du Rietz, and E. Williams, Interplay between Quantum Shells and Orientation in Quasifission, *Phys. Rev. Lett.* **113**, 182502 (2014).
- [28] K. Sekizawa and K. Yabana, Time-dependent Hartree-Fock calculations for multinucleon transfer and quasifission processes in the $^{64}\text{Ni} + ^{128}\text{U}$ reaction, *Phys. Rev. C* **93**, 054616 (2016).

- [29] J. Töke, R. Bock, G. X. Dai, A. Gobbi, S. Gralla, K. D. Hildenbrand, J. Kuzminski, W. F. J. Müller, A. Olmi, H. Stelzer, B. B. Back, and S. Björnholm, Quasi-fission: The mass-drift mode in heavy-ion reactions, *Nucl. Phys.* **A440**, 327 (1985).
- [30] D. J. Hinde, D. Hilscher, H. Rossner, B. Gebauer, M. Lehmann, and M. Wilpert, Neutron emission as a probe of fusion-fission and quasi-fission dynamics, *Phys. Rev. C* **45**, 1229 (1992).
- [31] E. Prasad, A. Wakhle, D. J. Hinde, E. Williams, M. Dasgupta, M. Evers, D. H. Luong, G. Mohanto, C. Simenel, and K. Vo-Phuoc, Exploring quasifission characteristics for $^{34}\text{S} + ^{232}\text{Th}$ forming ^{266}Sg , *Phys. Rev. C* **93**, 024607 (2016).
- [32] R. du Rietz, E. Williams, D. J. Hinde, M. Dasgupta, M. Evers, C. J. Lin, D. H. Luong, C. Simenel, and A. Wakhle, Mapping quasifission characteristics and timescales in heavy element formation reactions, *Phys. Rev. C* **88**, 054618 (2013).
- [33] C. Simenel, D. J. Hinde, R. du Rietz, M. Dasgupta, M. Evers, C. J. Lin, D. H. Luong, and A. Wakhle, Influence of entrance-channel magicity and isospin on quasi-fission, *Phys. Lett. B* **710**, 607 (2012).
- [34] A. S. Umar, C. Simenel, and W. Ye, Transport properties of isospin asymmetric nuclear matter using the time-dependent Hartree-Fock method, *Phys. Rev. C* **96**, 024625 (2017).
- [35] Z. Wu and L. Guo, Microscopic studies of production cross sections in multinucleon transfer reaction $^{58}\text{Ni} + ^{124}\text{Sn}$, *Phys. Rev. C* **100**, 014612 (2019).
- [36] A. Jedele, A. B. McIntosh, K. Hagel, M. Huang, L. Heilborn, Z. Kohley, L. W. May, E. McCleskey, M. Youngs, A. Zarrella, and S. J. Yennello, Characterizing Neutron-Proton Equilibration in Nuclear Reactions with Subzeptosecond Resolution, *Phys. Rev. Lett.* **118**, 062501 (2017).
- [37] E. Williams, K. Sekizawa, D. J. Hinde, C. Simenel, M. Dasgupta, I. P. Carter, K. J. Cook, D. Y. Jeung, S. D. McNeil, C. S. Palshetkar, D. C. Rafferty, K. Ramachandran, and A. Wakhle, Exploring Zeptosecond Quantum Equilibration Dynamics: From Deep-Inelastic to Fusion-Fission Outcomes in $^{58}\text{Ni} + ^{60}\text{Ni}$ Reactions, *Phys. Rev. Lett.* **120**, 022501 (2018).
- [38] C. Simenel, Particle-Number Fluctuations and Correlations in Transfer Reactions Obtained Using the Balian-Vénéroni Variational Principle, *Phys. Rev. Lett.* **106**, 112502 (2011).
- [39] V. E. Viola, K. Kwiatkowski, and M. Walker, Systematics of fission fragment total kinetic-energy release, *Phys. Rev. C* **31**, 1550 (1985).
- [40] D. J. Hinde, J. R. Leigh, J. J. M. Bokhorst, J. O. Newton, R. L. Walsh, and J. W. Boldeman, Mass-split dependence of the pre- and post-scission neutron multiplicities for fission of ^{251}Es , *Nucl. Phys.* **A472**, 318 (1987).
- [41] K. Godbey, C. Simenel, and A. S. Umar, Microscopic predictions for the production of neutron-rich nuclei in the reaction $^{176}\text{Yb} + ^{176}\text{Yb}$, *Phys. Rev. C* **101**, 034602 (2020).
- [42] J. A. Maruhn, P.-G. Reinhard, P. D. Stevenson, and A. S. Umar, The TDHF Code Sky3D, *Comput. Phys. Commun.* **185**, 2195 (2014).
- [43] B. Schuetrumpf, P.-G. Reinhard, P. D. Stevenson, A. S. Umar, and J. A. Maruhn, The TDHF code Sky3D version 1.1, *Comput. Phys. Commun.* **229**, 211 (2018).
- [44] K. Sekizawa and K. Yabana, Time-dependent Hartree-Fock calculations for multinucleon transfer processes in $^{40,48}\text{Ca} + ^{124}\text{Sn}$, $^{40}\text{Ca} + ^{208}\text{Pb}$, and $^{58}\text{Ni} + ^{208}\text{Pb}$ reactions, *Phys. Rev. C* **88**, 014614 (2013).
- [45] E. Chabanat, P. Bonche, P. Haensel, J. Meyer, and R. Schaeffer, A Skyrme parametrization from subnuclear to neutron star densities. Part II. Nuclei far from stabilities, *Nucl. Phys.* **A635**, 231 (1998).
- [46] D. Lacroix and S. Ayik, Stochastic quantum dynamics beyond mean field, *Eur. Phys. J. A* **50**, 95 (2014).